

MAHMOOD M. SALEH

ORCID: 0009-0006-6128-8273

Department of Physics, Faculty of Sciences, University of Sfax, Tunisia

E-mail: mms.82.2006@gmail.com, mahmood.m.saleh@otibaiji.oil.gov.iq

HAMADI KHEMAKHEM

ORCID: 0000-0002-1753-8451

Department of Physics, Faculty of Sciences, University of Sfax, Tunisia

E-mail: hamadi.khemakhem@fss.usf

ISHMAEL K. JASSIM

ORCID: 0009-0002-2997-6819

College of Medical Techniques, Al-Kitab University, Iraq

E-mail: prof.i.k.jassim@gmail.com

RAED HASHIM AL-SAQ

ORCID: 0000-0003-3538-457X

Directorate General of Education in the province of Nineveh, Ministry of Education, Iraq

E-mail: raed.h.alsaqa@st.tu.edu.iq

DOI: 10.15199/40.2024.6.2

Preparation and characterization of cermet MSZ/Ni-Al coating deposited by flame spraying technique

Przygotowanie i charakterystyka powłoki cermetalowej MSZ/Ni-Al osadzonej techniką natrysku płomieniowego

10MgO-ZrO₂/Ni-Al cermet powders were sprayed by flame spray technique onto low carbon steel substrates type API 5L used commonly in the oil industrial. The aim of the present study was to investigate the influence of the thermal treatment behaviour on the structural, mechanical and microstructural evolution properties in order to verify the thermal phase stability at high temperatures. The free-standing cermet samples (1.85 mm thick) were heat treated in air at 1000°C, 1100°C, 1200°C, 1300°C and 1350°C, respectively, for a 2 h aging time. The test properties were characterised by X-ray diffraction (XRD), scanning electron microscopy (SEM), energy dispersive spectroscopy (EDS), wear loss and Vickers hardness. The results showed that the deposited cermet coating became thicker and had ideal phase stability with the best mechanical properties when heat treated at 1300°C for 2 h of sintering. In addition, at 1350°C, the microstructure surface revealed split cracks and pores across the layers, which is not reliable for longer thermal stability. The results also showed that zirconium oxide (ZrO₂) undergoes a significant change from cubic (FCC-ZrO₂), tetragonal (T-ZrO₂) and monoclinic (M-ZrO₂) structures through the different temperature levels. These results also revealed that the wear loss value of the cermet coating is thus lower, and depends strongly on the porosity and hardness values. Finally, it can be concluded that the heat treatment at 1300°C (2 h) produces a typical uniform lamellar structure and high hardness values, which is reliable for longer thermal stability.

Keywords: thermal aging treatment, cermet coating, MSZ/Ni-Al system, thermal spray coating, mechanical properties

Na podłoża ze stali niskowęglowej typu API 5L, powszechnie stosowanej w przemyśle naftowym, naniesiono techniką natrysku płomieniowego proszek cermetalowy 10MgO-ZrO₂/Ni-Al. Celem badania było określenie wpływu obróbki cieplnej na właściwości strukturalne, mechaniczne i mikrostrukturalne powłok, aby zweryfikować stabilność fazy termicznej w wysokich temperaturach. Próbkę powłok cermetalowych (o grubości 1,85 mm) poddawano obróbce cieplnej w powietrzu w temperaturach 1000°C, 1100°C, 1200°C, 1300°C i 1350°C przez 2 h. Właściwości próbek oznaczono metodą dyfrakcji rentgenowskiej (XRD), skaningowej mikroskopii elektronowej (SEM) i spektroskopii rentgenowskiej z dyspersją energii (EDS), określono także zużycie ściernie i twardość Vickersa. Wykazano, że osadzona powłoka cermetalowa miała większą grubość i idealną stabilność fazową oraz najlepsze właściwości mechaniczne po 2 h spiekania w temperaturze 1300°C. Po obróbce cieplnej w temperaturze 1350°C na powierzchni mikrostruktury pojawiły się pory i pęknięcia w poprzek warstw, co nie sprzyja zapewnieniu stabilności termicznej w dłuższym czasie. Z badań wynika również, że tlenek cyrkonu (ZrO₂) w różnych temperaturach ulega znacznym zmianom: ze struktury sześciennej (FCC-ZrO₂) w tetragonalną (T-ZrO₂) i jednoskośną (M-ZrO₂). Uzyskane rezultaty świadczą także o tym, że zużycie powłoki cermetalowej jest mniejsze i silnie uzależnione od porowatości i twardości. W wyniku obróbki cieplnej w temperaturze 1300°C (przez 2 h) wytwarza się typowa jednolita struktura lamelarna i osiąga ona wysoką twardość, co jest konieczne do zapewnienia długotrwałej stabilności termicznej.

Słowa kluczowe: starzenie cieplne, powłoka cermetalowa, układ MSZ/Ni-Al, powłoka natryskiwana cieplnie, właściwości mechaniczne

■ Received / Otrzymano: 16.12.2023. Accepted / Przyjęto: 30.04.2024

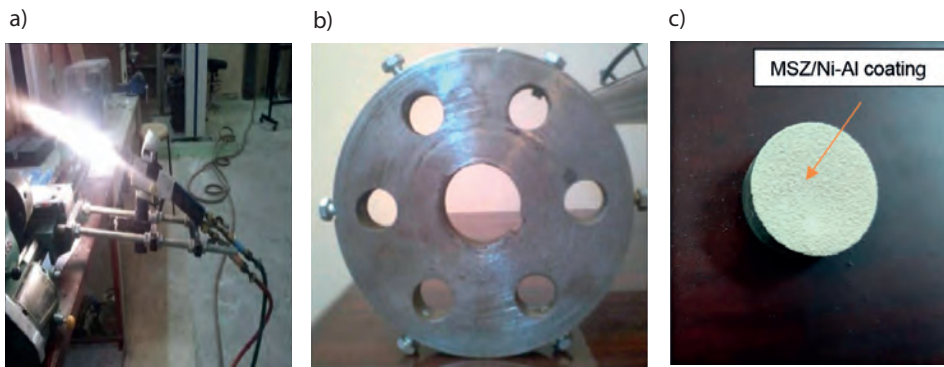


Fig. 1. The flame spray process during coating: a) flame spray device, b) turning holder, c) sample product

Rys. 1. Proces natryskiwania płomieniowego podczas powlekania: a) urządzenie do natryskiwania płomieniowego, b) uchwyt obrotowy, c) próbka produktu

1. Introduction

Thermal barrier ceramic coatings offer an attractive combination of structural and mechanical properties, including good thermal stability at high temperatures [1, 2]. The use of thermal barrier ceramic coatings can be useful in a wide range of applications to increase the service life of hot parts, oxidation resistance and protection of consumables by adding thick coatings, particularly on oil pipes in refineries [3, 4]. Partially stabilized zirconia ceramic (ZrO_2) exhibits excellent electrical and mechanical properties such as good wear resistance, high toughness, high melting point and excellent thermal resistance stability [5, 6]. Several researchers discovered that self-bonding metals such as Ni, Al, Cr, Co or alloys mixed with ceramic metal oxides such as Al_2O_3 , TiO_2 , ZrO_2 , WC and SiC undergo significant exothermic reactions between each other, improving bond strength, which provides the deposited coating, generally referred to as a cermet composite material, with a high adhesive force [7]. The flame spray coating technique is the most ideal and superior method to deposit thick cermet coatings and can be used for several engineering applications such as on turbine blades to provide protection from exposure to a high stable operating temperatures, or as oil pipe protection and thermal insulation [8]. Previously studied efforts using the yttria partially stabilized zirconia (YSM) system with self-bonding Ni-Co-Al metals do not yield successful results for high temperature operation [9, 10]. In this work, ceramic powders consisting of $10MgO-ZrO_2$ mixed with bonding $Ni_{50}-Al_{50}$ metal powders by means of the ball milling process, obtaining a nanoparticle size cermet composite of $10MgO-ZrO_2/Ni-Al$, named the MSZ/Ni-Al composite system, were sprayed by using the flame coating technique under optimum parameters to investigate the effect of heat treatment on phase stability, microstructure and wear resistance properties.

2. Materials and techniques

In this study, low carbon steel pipes (API 5L) used in the oil industry were used as a substrate. Tubes were cut as 26.5×26.5 mm square coupons with a thickness of 3.51 mm as substrate pieces. The substrate contained the chemical elements listed in Table 1. The substrates were sandblasted with Al_2O_3 with a particle size of $6 \mu m$ at a pressure of 5 bar. Sandblasting was performed at an angle of 70° and at a distance of 20 cm to ensure that a good roughness with the best adhesion was obtained. The substrates were first cleaned with alcohol, acetone, distilled water and dried using hot air. The flame spraying technique was carried out immediately after the cleaning (Rototec 80, Castoline Eutectic, Switzerland), as shown in Fig. 1a. Sample number 6 was fixed to holes on a rotating steel holder

(Fig. 1b). The commercial powders used to prepare the cermet coatings consisted of oxide ceramic powders ($10MgO-ZrO_2$) supplied by Sulzer-Metco with a particle size of $40-50 \mu m$ and partially stabilized with MgO. Nickel-aluminium powder with an average particle size of $55 \mu m$ was also used as a binder ($Ni_{50}-Al_{50}$; Amdry No. 995). Prior to spray coating, the initial morphology of both powders was determined by scanning electron microscopy (SEM) as shown in Fig. 2a, 2b. The raw cermet of the composite $10MgO-ZrO_2/Ni-Al$ powders, with a purity of 99.6%, was ball milled using a high energy planetary mill (homemade) consisting of stainless steel jars and 40 balls with a diameter of 10 mm. The rotational speed was 137 rpm. The ball to powder weight ratio was set at 40 : 1 gm. The new product sample after 1 h milling was 60 nm in size. The ideal parameters in the cermet coating process that produced optimized results are shown in Table 2. The cermet coating samples were isothermally heat treated in a high temperature chamber furnace (HTK 20/17, Bremen, Germany) at different temperatures of $1000^\circ C$, $1100^\circ C$, $1200^\circ C$, $1300^\circ C$ and $1350^\circ C$, respectively, for a 2 h aging time. The samples were heated at approximately $10^\circ C/min$ to the target temperature and then cooled naturally to room temperature in a side furnace. The cermet coating sample was also heat treated at $1300^\circ C$ for 6 h in the furnace to check the influence of time aging on thermal phase stability and mechanical properties. The thermal stability was also investigated by differential scanning calorimetry (DSC; Netzsch 404, Germany) at a rate of $5^\circ C \text{ min}^{-1}$ up to $1750^\circ C$.

Table 1. Chemical composition of oil pipe substrate

Tabela 1. Skład chemiczny rurociągu do transportu ropy naftowej

Element	C	Mn	P	S	Cu	Ni	Cr	Mo	V
Weight%	0.30	1.20	0.05	0.045	0.40	0.40	0.40	0.15	0.08

Table 2. The ideal flame spray parameters of the cermet coating MSZ/Ni-Al

Tabela 2. Optymalne parametry natrysku płomieniowego powłoki cermetowej MSZ/Ni-Al

Operating parameters	Values
Spray distance	20 cm
Flame spray temperature	$\approx (3000)^\circ C$
Maximum thickness	1.850 mm
Particle size of $MgO-ZrO_2$	$40-50 \mu m$
Particle size of $Ni_{50}-Al_{50}$	$55 \mu m$
Oxygen pressure	5–6 bar
Acetylene pressure	2–3 bar
Angle of sand blasting	70°
Rotation number	5
Oxy-acetylene mixing	3 : 1

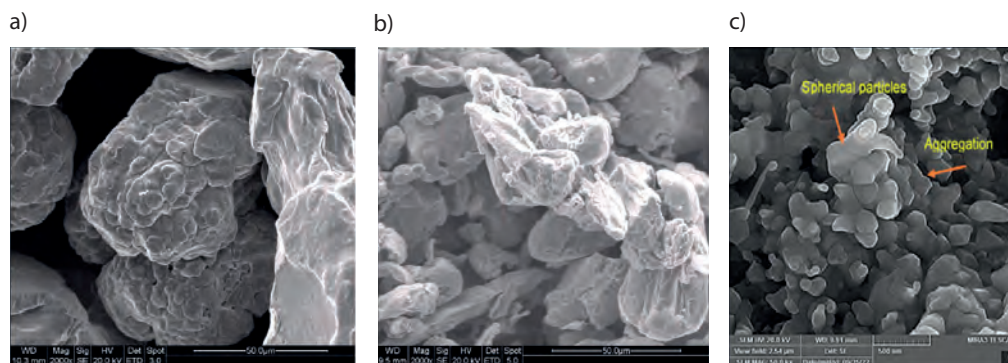


Fig. 2. SEM morphology for initial powders used: a) ceramic MgO-ZrO_2 , b) $\text{Ni}_{50}\text{-Al}_{50}$ alloy bond, c) cermet coating of $\text{MgO-ZrO}_2/\text{Ni-Al}$ at RT by flame spraying method

Rys. 2. Morfologia SEM zastosowanych proszków wyjściowych: a) ceramiczny MgO-ZrO_2 , b) spoiwo stopowe $\text{Ni}_{50}\text{-Al}_{50}$, c) powłoka cermetalowa $\text{MgO-ZrO}_2/\text{Ni-Al}$ przed obróbką, nałożona metodą natryskiwania płomieniowego

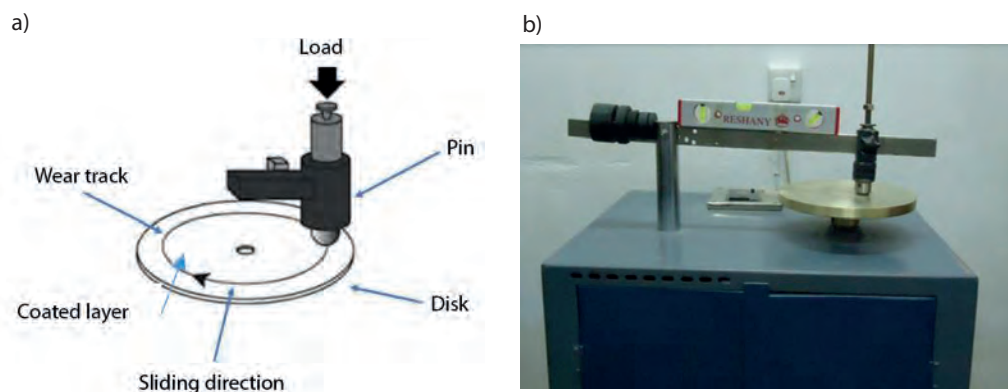


Fig. 3. Wear test of cermet coating MSZ/Ni-Al: a) wear pin-on-disc machine, b) schematic diagram of the wear test

Rys. 3. Test zużycia powłoki cermetalowej MSZ/Ni-Al: a) urządzenie do badania zużycia ściernego, b) schemat testu zużycia

Source: [6, p. 146].

Źródło: [6, s. 146].

The structural and phase transformations were carefully studied by X-ray diffraction (XRD) in a Philips diffractometer using filtered Cuka radiation ($\lambda = 1.540\text{\AA}$). The goniometer was set to a scan rate of $0.05^\circ/\text{s}$ over a range of 2θ . The microstructure and morphology of the cermet composite powder particles and as-sprayed coatings at different temperature ranges were investigated using a scanning electron microscope (SEM) equipped with an energy dispersive X-ray (EDAX) analyzer. A Jeol JIB-46 IOF SEM was used. The microhardness of the surface coating values (HV) was determined by the average of 5 tests at a load of 100 gm during a 15 s period. A microhardness tester (Leitz Wetzlar, Germany) was used after smoothing and polishing the coating surface. Finally, the pin-on-disc wear test method was used. The steel rotating disc of hardness HV 40 was used under constant load (9 N) and sliding distance (1200 cm/min) as shown in Fig. 3. The specimens were weighed before and after each test using an electronic scale with an accuracy of 0.002 g, and the losses were recorded.

3. Results and discussion

The composition of the two raw materials used was first investigated prior to spray coating (Fig. 2). It shows the SEM microstructure of 10MgO-ZrO_2 powder and $\text{Ni}_{50}\text{-Al}_{50}$ powder, respectively. Fig. 2a reveals large agglomerates of spherical particles formed in a uniform homogeneous state, while Fig. 2b appears to have sub-angular particles whose size of $\text{Ni}_{50}\text{-Al}_{50}$ is about $50\text{--}55\ \mu\text{m}$, while that of 10MgO-ZrO_2 is about $40\text{--}50\ \mu\text{m}$. The micrograph of the cermet coating after ball milling for 1 h (Fig. 2c) shows that the MSZ/Ni-Al particles are spherical and uniform in size at a spray distance of 20 cm.

Fig. 4a–4e show SEM micrographs of MSZ/Ni-Al surface cermet coating at different heat treatment high temperature values: 1000°C , 1200°C , 1300°C , 1350°C , respectively, at a sintering time of 2 h. In Fig. 4a the morphology of the cermet surface coating under

heat treatment of 1000°C at a sintering time of 2 h is shown. The surface coating reveals a high uniform spherical particle distribution of ZrO_2 grains which constituted agglomerates with a grain size around ($45\text{--}55\ \mu\text{m}$). The grains of MgO, Ni-Al and ZrO_2 appear to be strongly sintered at 1000°C . Also, the results of the sample heat treated at 1100°C (Fig. 4b) indicate that the surface coating is similar to that treated at 1000°C . It shows that most of the MSZ/Ni-Al particles also produce spherically uniform agglomerates everywhere homogeneously on the surface coating [11]. When the heat treatments reach 1200°C , it is observed that the grains are also homogeneously distributed, with small and large agglomerated microstructures observed among all grain sizes of MgO, Ni-Al and ZrO_2 particles (Fig. 4c). Further treatment of Al at 1300°C yields a high increment of grain growth which constitutes a significant departure from the other treated samples (Fig. 4d). No substantial trace of pores or cracks appeared. It is clear that the steady state for particle size distribution has almost been achieved thanks to a balance with more uniform particle size and strongly formed agglomerates (Fig. 4d). Moreover, at 1350°C treatment spallation, visible pores and cracks were observed on the surface coating as clearly is shown in Fig. 4e. Fig. 4f reveals the SEM morphology structure of the cermet coating MSZ/Ni-Al system at small scale ($2\ \mu\text{m}$), which was taken for greater accuracy, and clearly shows spallation and surface defects [12]. The results also show that the grain size growth started to increase gradually during the increasing heat treatment up to 1350°C and then suddenly decreased due to surface cleavage and formation of several pores with crack propagation on the top surface of the cermet coating (Fig. 5). The results obtained between 1000°C and 1300°C are clearly linked to the effect of heat treatment on the high growth rate [13]. Fig. 5a also reveals that the grain size of the MSZ/Ni-Al composite cermet coating during treatment at 1300°C is more than two times larger (2.478) than when heated at 1000°C , which indicates that the sample

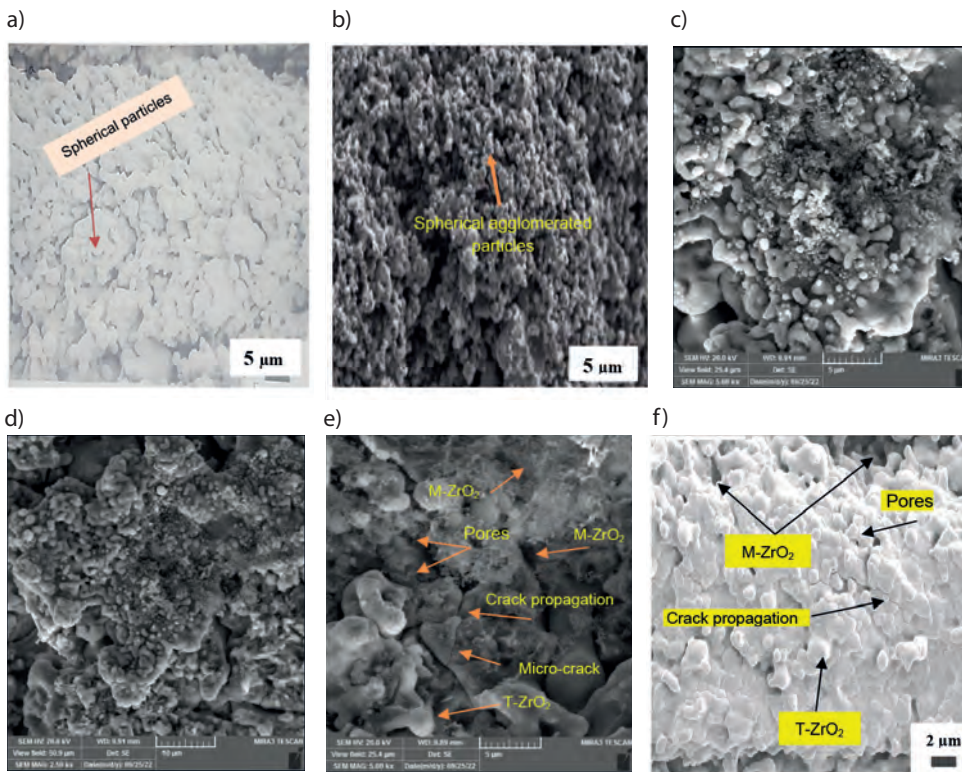


Fig. 4. SEM micrographs of MSZ/Ni-Al surface cermet coatings at different temperature values for 2 h sintering time: a) 1000°C, b) 1100°C, c) 1200°C, d) 1300°C, e) 1350°C, scale 5 μm, f) 1350°C, scale 2 μm
 Rys. 4. Mikrofotografie SEM powierzchni powłok cermetalowych MSZ/Ni-Al po 2 h spiekania w różnych temperaturach: a) 1000°C, b) 1100°C, c) 1200°C, d) 1300°C, e) 1350°C, skala 5 μm, f) 1350°C, skala 2 μm

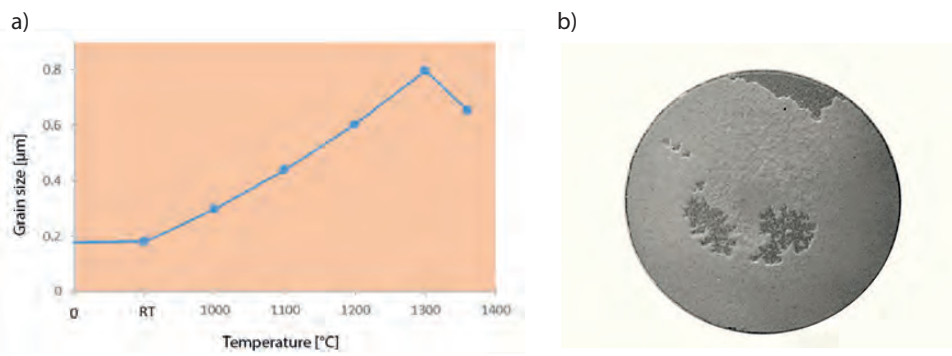


Fig. 5. Tests results: a) the relationship between the grain sizes and heat treatment temperatures of surface composite MSZ/Ni-Al coating, b) photograph of sample treated at 1350°C for 2 h sintering time
 Rys. 5. Wyniki badań: a) zależność między wielkością ziaren a temperaturą obróbki cieplnej powierzchni kompozytowej powłoki MSZ/Ni-Al, b) fotografia próbki po 2 h spiekania w temperaturze 1350°C

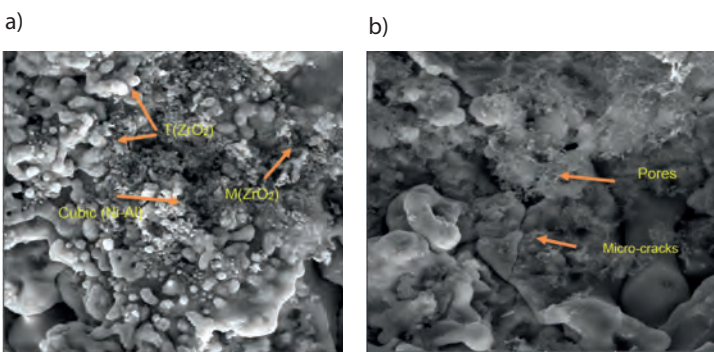


Fig. 6. SEM micrographs of cermet MSZ/Ni-Al surface coatings after treatment at 1300°C as a function of sintering time: a) 6 h, b) 7 h
 Rys. 6. Mikrofotografie SEM cermetalowych powłok powierzchniowych MSZ/Ni-Al po spiekaniu w temperaturze 1300°C przez: a) 6 h, b) 7 h

treated at 1300°C has a significantly improved uniform microstructure, high adhesion force between layers and high thickness ≤1.85 mm, which gives a great advantage especially in high thermal stability applications [13, 14].

Some other tests were repeated at a heat treatment temperature of 1300°C for 6–7 h to see the effect of sintering time on the microstructural properties of the cermet coating of the MSZ/Ni-Al system (Fig. 6). The results showed that after 6 h of sintering, the cermet coating had an atypical structure without any trace of surface defects (Fig. 6a). For the heat treatment of 7 h, the sintering time was

used to check the thermal stability of the sample. It appears that degeneration occurs in the surface coating with micropores, which are dominated as result in a long sintering time 7 h effect (Fig. 6b).

Energy dispersive X-ray analysis (EDX) experiments have been conducted on the cermet coating samples at various thermal treatment temperatures: 1000°C and 1350°C (Fig. 7, Table 3). It is evident that only the peaks of Zr, Mg, Ni, Al and O with traces of Cr are observed for both samples. In fact, the presence of Cr elements results from it being added by the manufacturer to increase the adhesion force between the elements of the cermet coating [15].

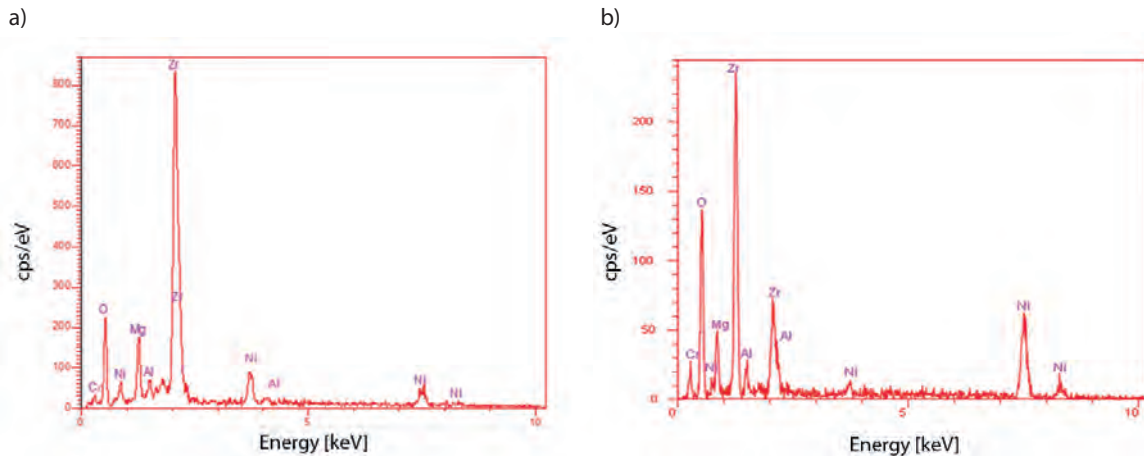


Fig. 7. EDX patterns for cermet coating MSZ/Ni-Al system at various temperatures: a) 1000°C, b) 1300°C

Rys. 7. Wykresy EDX dla powłoki cermetalowej MSZ/Ni-Al w różnych temperaturach: a) 1000°C, b) 1300°C

The results also show that the weight percentage (wt%) for all elements in both treated samples is very similar. This means that the raw materials used in this study are of high purity and the accuracy of the tests is high. A comparison of the two samples treated at 1000–1300°C revealed that the samples possess agglomerated spherical particle distributions (Fig. 6). This agglomeration may result in a more homogeneous structure due to the interaction between the MgO-ZrO₂/Ni-Al particles, providing much improved mechanical and structural properties. Indeed, the sample treated at 1300°C for 6 h sintering time was more successful in providing strong thermal stability.

The structural properties of the cermet coating under different heat treatment temperatures: RT, 1000°C, 1100°C, 1200°C and 1300°C, for a sintering time of 2 h were analyzed by XRD (Fig. 8). Fig. 8f shows the sample treated at 1300°C for 6 h to see the effect of sintering time on the structural properties of the MSZ/Ni-Al coating. Before coating, the cermet powders (RT) show four phases, obviously corresponding to the cubic FCC-ZrO₂ and tetragonal T-ZrO₂ phases. The other two phases belong to the cubic FCC-MgO and FCC-self bonding Ni-Al phases. All peaks are clearly small in intensity, with broader peaks (Fig. 8). The powder samples after coating and treatment at 1000°C for 2 h sintering time show that the peaks at high (2θ) angles are still broader with small intensity, but at small angles of 2θ ≈ 35° they are characterized by high intensity of the T-ZrO₂ phase for all the different heat treatments used. The diffraction peaks related to the FCC-ZrO₂ and T-ZrO₂ phases are still dominant during the heat treatment up to 1300°C for a sintering time of 2 h (Fig. 8). The results also show that the phases increase significantly with increasing heat treatment temperatures. The peak intensity of the cermet MSZ/Ni-Al coating at 2θ ≈ 35.30° with the T-ZrO₂ phase appears to be much stronger than the other phases. It is also interesting to study the effect of sintering time to check the thermal stability at high temperatures (1300°C) as a function of sintering time (6 h), as shown in Fig. 8f; a split peak at a high angle around 2θ ≈ 71° starts to increase from the initial treatment (1000°C) to the severity state at the 1300°C treatment at a sintering time of 6 h. This splitting phenomenon was observed and accompanied by the total loss of the FCC-ZrO₂ phase at the 2θ angles of 45° and 65°, respectively (Fig. 8e, 8f). The splitting peak actually has two peaks in the same position. The X-ray analysis revealed the appearance of a new monoclinic phase M-ZrO₂ together with T-ZrO₂.

Table 3. Elemental composition analysis by EDX processing at 1000°C and 1350°C for MSZ/Ni-Al coating

Tabela 3. Analiza składu pierwiastkowego powłoki MSZ/Ni-Al metodą EDX w temperaturze 1000°C i 1350°C

Temperature [°C]	Element	Energy level	Weight%	Total [%]
1000	O	K	27.95	99.97
	Zr	L	51.21	
	Mg	K	9.67	
	Ni	K	5.18	
	Al	K	5.96	
1300	O	K	29.66	99.51
	Zr	L	55.12	
	Ni	L	7.91	
	Al	L	6.82	

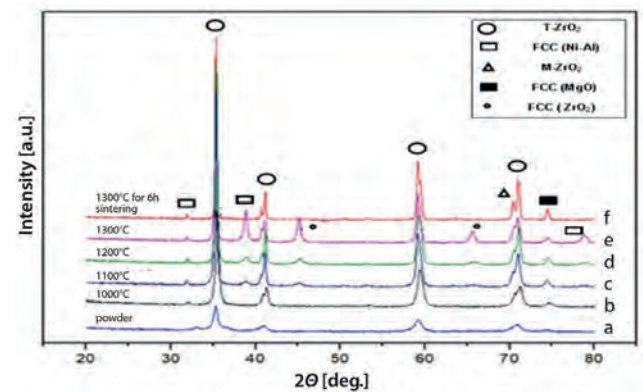


Fig. 8. XRD structural analysis at various heat treatment of cermet coating MSZ/Ni-Al as a function of treatment temperatures at 2 h sintering time: a) powder, b) 1000°C, c) 1100°C, d) 1200°C, e) 1300°C, f) 1300°C for 6 h sintering

Rys. 8. Analiza strukturalna XRD powłoki cermetalowej MSZ/Ni-Al po spiekaniu przez 2 h w różnych temperaturach: a) proszek, b) 1000°C, c) 1100°C, d) 1200°C, e) 1300°C, f) 1300°C po spiekaniu przez 6 h

This may be due to the treatment at 1300°C for 6 h of sintering, which is sufficient treatment to intensify T-ZrO₂ and M-ZrO₂ phases, giving them the best thermal stability. Finally, the X-ray peaks for all the samples measured under different treatments do not show any trace of foreign elements, as impurity phases have been detected. This result is in fact identical to that obtained by EDX, which also indicates no impurities.

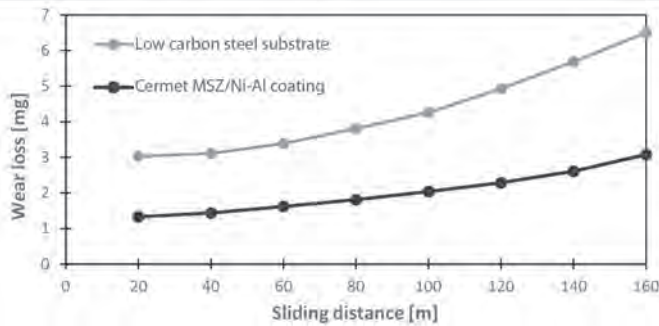


Fig. 9. Wear loss relation to the sliding distance at 9 N normal load effect

rys. 9. Zależność zużycia od drogi poślizgu przy normalnym obciążeniu 9 N

Finally, the results of the effective variable heat treatment temperatures at 2 h sintering time on the mechanical properties (porosity, hardness, grain size) of the cermet 10MgO-ZrO₂/Ni-Al (MSZ/Ni-Al) coating are summarized in Table 4. The microhardness (HV) results clearly revealed that there is no major change when the heat treatment is varied from 1000°C to 1300°C with a sintering time of 2 h, which is likely due to the fact that all the particles of the composite cermet coating are formed and completely melted in a homogeneous structure [11]. The results also observed at the same time showed a small change in the magnitude of the thickness and porosity percentage values during the treatment processes, which amounted to ca. 1.854 mm thickness and 7.480% porosity with the cermet the sample treated at 1300°C for 2 h of sintering. This means that a thick cermet coating can improve the structural and mechanical properties of the low carbon steel substrate of the oil pipes used in this study when exposed to an erosive environment at 1300°C, which has been shown to be the most suitable in providing the best thermal stability and is ideal for longer temperature life.

The microhardness is in fact directly dependent on the porosity percentage, which was found to be about 7.48% after heat treatment at 1300°C. This may be due to the presence of oxides related to MgO, ZrO₂, NiO and Al₂O₃ oxides between the coating layers. As the heating temperature continued to increase to 1350°C, a significant decrease in hardness value was observed. We believe that the increased cracking, porosity and other surface defects led to the reduction in hardness, as shown by the SEM results (Fig. 4), which reveals many defects with porosity. The results also clearly show the influence of the heat treatment on the grain sizes of the MSZ and Ni-Al samples (Table 4). It is evident that the grain size growth began to increase with increasing heat treatment up to 1300°C, indicating the link between high temperature treatment and high growth. This may be related to the reduction in porosity values associated with the increase and improvement in structural, microstructural and mechanical properties [16]. The wear loss amount is related to the sliding distance at 9 N load effect on the low carbon steel oil pipe substrate and into the 10MgO-ZrO₂/Ni-Al cermet coating sample (Fig. 9). The results show that the wear loss value of the simple cermet coating on the substrate is lower probably due to the fact that the hardness value of the low carbon steel substrate is much lower than that of the cermet coating sample. In our wear loss results for the cermet coating, we found a very strong wear loss dependence on the porosity percentage and hardness values. The highest hardness value of 47.85 HV was observed at the lowest porosity percentage of 7.48%, while the lowest wear loss

Table 4. Mechanical properties of the cermet 10MgO-ZrO₂/Ni-Al (MSZ/Ni-Al) coating after 2 h sintering time at various temperatures

Tabela 4. Właściwości mechaniczne powłoki cermetalowej 10MgO-ZrO₂/Ni-Al (MSZ/Ni-Al) po 2 h spekania w różnych temperaturach

Temperature [°C]	Porosity [%]	Microhardness [HV]	Grain size [μm]
1000	9.86	46.88	0.322
1100	8.89	46.98	0.412
1200	8.04	47.46	0.605
1300	7.48	47.85	0.798
1350	13.77	25.27	0.491

of approximately 3×10^{-3} mg was observed at the normal load of 9 N (Fig. 9).

4. Conclusion

Cermet mixtures of ceramic 10MgO-ZrO₂ oxide powder with bonding metal Ni₅₀-Al₅₀ alloy powder were deposited by the flame spray technique. The cermet sample 10MgO-ZrO₂ + Ni-Al coatings were subjected to heat treatment sintering for 2 h at different temperatures (1000°C, 1100°C, 1200°C, 1300°C and 1350°C) in order to study the influence of high temperature ranges on their structural, microstructural and mechanical properties. XRD analysis revealed that the cermet MSZ/Ni-Al powders before coating (RT) contain four phases: FCC-MgO, FCC(Ni-Al), FCC-ZrO₂ and the tetragonal phase T-ZrO₂ at different initial temperatures for a sintering time of 2 h. The thermal stability at high temperatures (1300°C) was checked by increasing the sintering time to 6 h. A splitting peak at high angle was observed with the FCC-ZrO₂ phase completely losing, and a new monoclinic phase M-ZrO₂ sharing the phase with the T-ZrO₂ phase to produce the best thermal stability. The micrograph (SEM) of the MSZ/Ni-Al surface coating reveals highly uniform spherical particle distributions that form agglomerates up to 1300°C. Above that, at 1350°C treatment, spallation, pores and cracks were clearly observed. The effect of variable heat treatment on mechanical properties was also observed, with no significant change in microhardness when the heat treatment temperature is varied up to 1300°C. There was also a sudden reduction in hardness value to 25.27 HV at 1350°C treatment. The thickness and porosity values during heat treatment at 1300°C are 1.854 mm and 7.480%, respectively. We also noted the highest hardness value of 47.85 HV with the lowest wear loss of approximately 3×10^{-3} mg at 9 N normal load. In conclusion, this result means that the cermet coating MSZ/Ni-Al composite system sintered at 1300°C for 6 h can improve its structural and mechanical properties to protect the low carbon steel of oil pipes at higher temperatures.

Acknowledgments

The researchers are grateful to the North Refineries Company, Baiji, Iraq, for collaborating with the University of Tikrit in providing the necessary facilities in the Materials Engineering Laboratory. Special thanks are also due to the technical support provided over the past two years, in particular to Engineer Khamis and Mr Salam in the Mechanical and Rotating Equipment Department, and to the Iraqi Ministry of Science and Technology for allowing the use of flame spraying, SEM, EDX, XRD and microhardness equipment.

CRediT authorship contribution statement

Mahmood M. Saleh: Data curation, Investigation, Methodology, Project administration, Resources, Software, Supervision, Validation, Visualization, Writing – original draft, Writing – review & editing.

Hamadi Khemakhem: Data curation, Supervision.

Raed Hashim Al-Saqa: Formal analysis, Investigation, Project administration, Resources, Software, Validation, Writing – original draft, Writing – review & editing.

Ishmael K. Jassim: Funding acquisition.

BIBLIOGRAPHY

- [1] M. M. Khalaf, H. Ibrahimov, E. H. Ismailov. 2012. "Nanostructured Materials: Importance, Synthesis and Characterization – A Review." *Chemistry Journal* 2(3): 118–125.
- [2] L. M. Silva, M. A. Morales, J. F. M. L. Mariano, J. A. H. Coaquira, J. H. de Araújo. 2023. "Synthesis, Structural and Magnetic Study of BaFe₁₂O₁₉/CoFe₂O₄@CoFe₂ Nanocomposites." *Journal of Alloys and Compounds* 963: 171285. DOI: 10.1016/j.jallcom.2023.171285.
- [3] S. Lan, M. A. Willard. 2017. *Synthesis of Soft Magnetic Nanomaterials and Alloys*. In: Y. Hou, D. J. Sellmyer (eds.). *Magnetic Nanomaterials: Fundamentals, Synthesis and Applications*. Weinheim: Wiley.
- [4] C. Suryanarayana. 2001. "Mechanical Alloying and Milling." *Progress in Materials Science* 46(1–2): 1–184. DOI: 10.1016/S0079-6425(99)00010-9.
- [5] L. Aymard, B. Dumon, G. Viau. 1996. "Production of Co-Ni Alloys by Mechanical Alloying." *Journal of Alloys and Compounds* 242(1–2): 108–113. DOI: 10.1016/0925-8388(96)02285-2.
- [6] I. K. Jassim, K.-U. Neumann, D. Visser, P. J. Webster, K. R. A. Ziebeck. 1992. "The Magnetic Structure of the Heusler Alloy Pd_{2-x}Ag_xMnIn." *Physica B: Condensed Matter* 180–181(1): 145–146. DOI: 10.1016/0921-4526(92)90688-O.
- [7] A. Mukhtar, T. Mehmood, K. M. Wu. 2017. "Investigation of Phase Transformation of CoNi Alloy Nanowires at High Potential." *Materials Science and Engineering* 239: 012017. DOI: 10.1088/1757-899X/239/1/012017.
- [8] B. Neelima, N. V. Rama Rao, V. Rangadhara Chary, S. Pandian. 2015. "Influence of Mechanical Milling on Structure, Particle Size, Morphology and Magnetic Properties of Rare Earth Free Permanent Magnetic Zr₂Co₁₁ Alloy." *Journal of Alloys and Compounds* 661: 72–76. DOI: 10.1016/j.jallcom.2015.11.186.
- [9] A. Y. Khidhaeir, I. K. Jassim. 2023. "Fabrication and Characterization of Binary Fe₆₀-Co₄₀ Alloy by Powder Metallurgy Method." *International Journal of Scientific Research in Science and Technology* 10(5): 391–396. DOI: 10.32628/IJSRST52310528.
- [10] H. Shokrollahi. 2009. "The Magnetic and Structural Properties of the Most Important Alloys of Iron Produced by Mechanical Alloying." *Materials and Design* 30(9): 3374–3387. DOI: 10.1016/j.matdes.2009.03.035.
- [11] M. Khajepour, S. Sharafi. 2012. "Characterization of Nanostructured Fe-Co-Si Powder Alloy." *Powder Technology* 232: 124–133. DOI: 10.1016/j.powtec.2012.07.051.
- [12] M. E. McHenry, D. E. Laughlin. 2014. *Magnetic Properties of Metals and Alloys*. In: D. E. Laughlin, K. Hono (eds.). *Physical Metallurgy*. Amsterdam: Elsevier.
- [13] H. M. K. Frage, I. K. Jassim, J. A. Yagoob. 2022. "Synthesis and Characterization of Binary Ni₇₅-Co₂₅ Alloy by Mechanical Alloying." *International Journal of Mechanical Engineering* 7(2): 697–702.
- [14] H. A. F. Al-Falahi, E. Hameed. 2019. "Preparing and Improving the Properties of Sodium Acrylate Polymer by Adding Dentonite for the Treatment of Desertification Phenomenon." *Al-Kitab Journal for Pure Sciences* 3(1): 15–29. DOI: 10.32441/kjps.03.01.p2.
- [15] R. A. Raimundo, V. D. Silva, L. S. Ferreira, F. J. A. Loureiro, D. P. Fagg, D. A. Macedo, U. U. Gomes, M. M. Soares, R. M. Gomes, M. A. Morales. 2023. "NiFe Alloy Nanoparticles Tuning the Structure, Magnetism, and Application for Oxygen Evolution Reaction Catalysis." *Magnetochemistry* 9(8): 201. DOI: 10.3390/magnetochemistry9080201.
- [16] M. M. Saleh, H. Khemakhem, I. K. Jassim, R. H. Al-Saqa. 2024. "Structure and Mechanical Properties of Cermet Ni-Al/MSZ Thick Coating Prepared by Flame Spraying Technique." *Ochrona przed Korozją* 1(67): 9–14. DOI: 10.15199/40.2024.1.2.

WYDAWNICTWO SIGMA-NOT

ponad 70 LAT NA RYNKU

34 TYTUŁY

150 000 PUBLIKACJI

Bądź bardziej EKO

KORZYSTAJ Z ZASOBÓW
PORTALU INFORMACJI TECHNICZEJ

in
ig
fb

QR code



We protect and
beautify the world™

**Budynki produkcyjne
i publiczne**

ul. Łużycka 8A
81-537 Gdynia
tel. 58 774 99 00
fax 58 774 99 01
customers@ppg.com